NRIAG JOURNAL OF ASTRONOMY AND GEOPHYSICS
2022, VOL. 11, NO. 1, 293–305
https://doi.org/10.1080/20909977.2022.2094530

Subgrade soil evaluation using integrated seismic refraction tomography and geotechnical studies: A case of Ajaokuta-Anyigba Federal highway, North-Central Nigeria

Obasaju Daniel Opemipo [a], Oloruntola Moroof [b], Oladele Sunday [b], Ojekunle Victor [b] and Baiyegunhi Christopher [c]

[a]Department of Earth Sciences, Kogi State University, Anyigba, Nigeria; [b]Department of Geosciences, University of Lagos, Lagos, Nigeria; [c]Department of Geology and Mining, University of Limpopo, Sovenga, Limpopo Province, South Africa

ABSTRACT

Integrated seismic refraction tomography (SRT) and geotechnical tests were conducted on failed and stable sections of the Ajaokuta – Anyigba Highway, North-central Nigeria. This study was aimed at characterising the soil profile, determining the competence of the subgrade soils, and establishing relationships between geophysical and geotechnical parameters. Primary wave velocities (Vp) were calculated by using SeisImager/2D (V.2.9.1). The subgrade soils of the unstable segment were characterised by low Vp (358–607 m/s) while higher Vp (762–1417 m/s) characterised the stable segment. The geotechnical results confirmed the seismic refraction results. Geotechnical results revealed that the subgrades of the unstable section are generally classified as A-6 and A-7-6 clayey soils, with low to high plasticity, and a fair to poor subgrade rating. While the subgrades of the stable section are grouped as A-2-4 silty sands with low compressibility and good to excellent subgrade ratings. Simple linear regression analysis showed fairly strong positive correlations between Vp and sand with CBR (r = 0.81 and 0.78, respectively). On the other hand, fairly strong negative correlations were obtained between Vp and the plasticity index with fines (r = −0.63 and −0.82 respectively).

ARTICLE HISTORY
Received 26 January 2022
Revised 29 April 2022
Accepted 22 June 2022

KEYWORDS
Primary wave velocity (Vp); seismic refraction tomography (SRT); geotechnical parameters; linear regression; subgrade soils

1. Introduction

A key area in engineering geological and geotechnical engineering investigation is the stability of structures such as roads, bridges, buildings, slopes, tunnels, and dams (Roodposhti et al. 2019). The knowledge of the engineering properties of the foundation soils is paramount for successful construction and design. The information obtained from geotechnical investigations is particularly applicable to the points' tested. The assumption by geotechnical engineers that the result of a test point in an area could be used for other parts of the same area might prove disastrous, because of the inhomogeneity of the earth's surface. This is partly responsible for failed structures in various parts of Nigeria. In the same vein, the cost of conducting geotechnical tests at several points over a large area is not only enormous but also invasive and time-consuming. Among other geophysical methods, the seismic refraction survey has been shown by several researchers as an efficient alternative and also an aid to the geotechnical investigation because it is less time-consuming and cost-effective (Adegbola et al. 2012; Mohammed et al. 2013; Al-Saigh and Al-Heety 2014; Ilori et al. 2014; Khalil and Hanafy 2016; Pegah and Mahmoodi 2016; Adewoyin et al. 2017; Allo et al. 2019; Izumotani et al. 2020). Aka et al. (2018) studied the competence of shallow subsoils as foundation materials for construction purposes in South-Eastern Nigeria by using seismic refraction. Weak formations characterised by low P-wave velocity were determined to be the major cause of highway failure and structural defects. A seismic refraction survey is an in-situ test that can help to evaluate the stiffness properties of subsoils in an undisturbed state as well as aid in unravelling near-surface structures and soil layering (Pegah and Mahmoodi 2016). Furthermore, it can provide reliable information about the velocity distribution in different layers of earth materials, depth to underlying layers, and bedrock structure (Azwin et al. 2013). According to Steeples and Miller (1990), the earth's materials' mechanical properties are easily deciphered by the seismic method but are insensitive to their chemistry and fluid content. When seismic energy is generated from a source at the earth's surface, it becomes refracted as it travels through the layers at the boundary between two media of varying impedance (Kearey et al. 2002; Reynolds 2011). Geophones fixed at intervals from the source of the energy sense the waves and record their varying times of arrival, which are displayed by the seismograph. The times of arrival of the waves in relation to the distance helps determine the velocity of the waves,

CONTACT Obasaju Daniel Opemipo obasajudaniel@gmail.com Department of Earth Sciences, Kogi State University, Anyigba, Nigeria

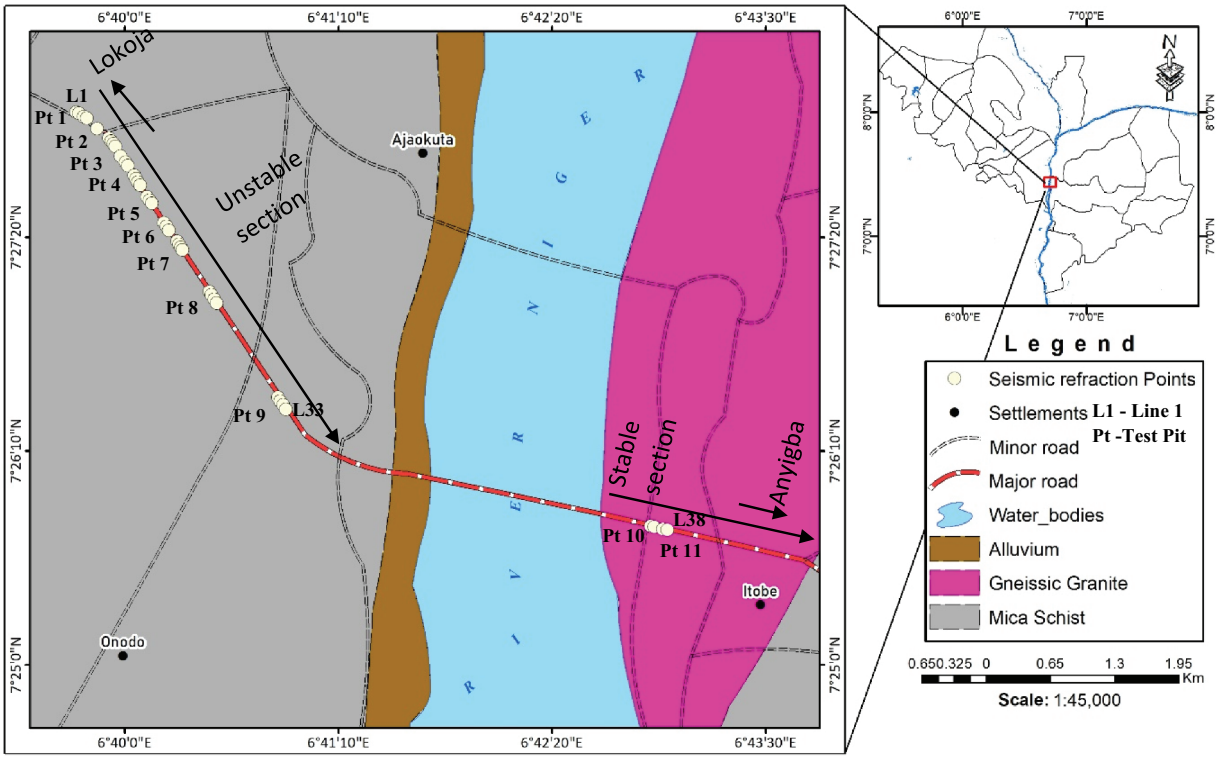

Figure 1. Geologic Map of the study area showing the Ajaokuta-Anyigba highway (Modified from Onimisi et al. 2013).

which in turn provides a clue about the nature of the subsurface layers and their stiffness or degree of compaction. The success of seismic refraction in site investigations such as highways depends on the fact that different subsurface earth layers have varying velocities. This is a function of their density and degree of compaction. It is capable of providing variation in the subsurface velocity both laterally and vertically and therefore reflects variation in the earth's subsurface geology in two dimensions. Seismic refraction tomography adopted in this study helped to image the subsurface geology rapidly by providing the P-wave distribution of the earth materials both laterally and vertically, which is in agreement with the work of Pegah and Mahmoodi (2016). Furthermore, it is a viable method in areas with strong lateral velocity gradients and where little or no prior knowledge of subsurface structure is available (Optim 2001).

The highway is an important engineering structure that consists of subsoil layers that include the subgrade, subbase, and base course in flexible pavement designs. Subgrade soil is the foundation soil and is a product of the in-situ weathering of the basement rock (in the Basement Complex environment). It is therefore a product of geology and the climatic factor of an environment. Unfortunately, geological factors are rarely considered in the construction and rehabilitation of several highways in Nigeria, even though the subgrade soil is a product of geology (Adeyemi et al. 2014). The causes of the continuous failure of highways in Nigeria are not adequately investigated before rehabilitation (Adeyemi et al. 2014). Sources of highway failure have always been attributed to the use of poor construction materials, traffic loading, and poor design (Jegede 2004; Ogundipe 2008; Okigbo 2012). Similar causes of failure are often proposed irrespective of the geology of the area. A few studies have, however, shown the influence of geology on the stability and otherwise of highways. Research by Oladapo et al. (2008) and Okpoli and Bamidele (2016) revealed that highway failure could be precipitated by geological features, which include faults and clayey subgrades.

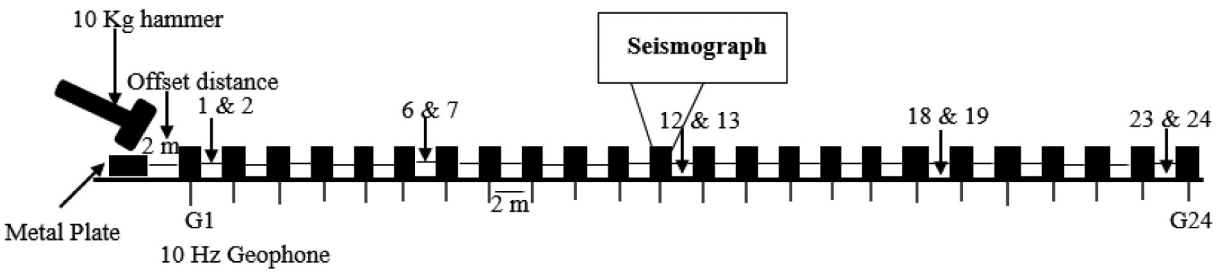

Figure 2. Field Set up for five-shot points for seismic refraction.

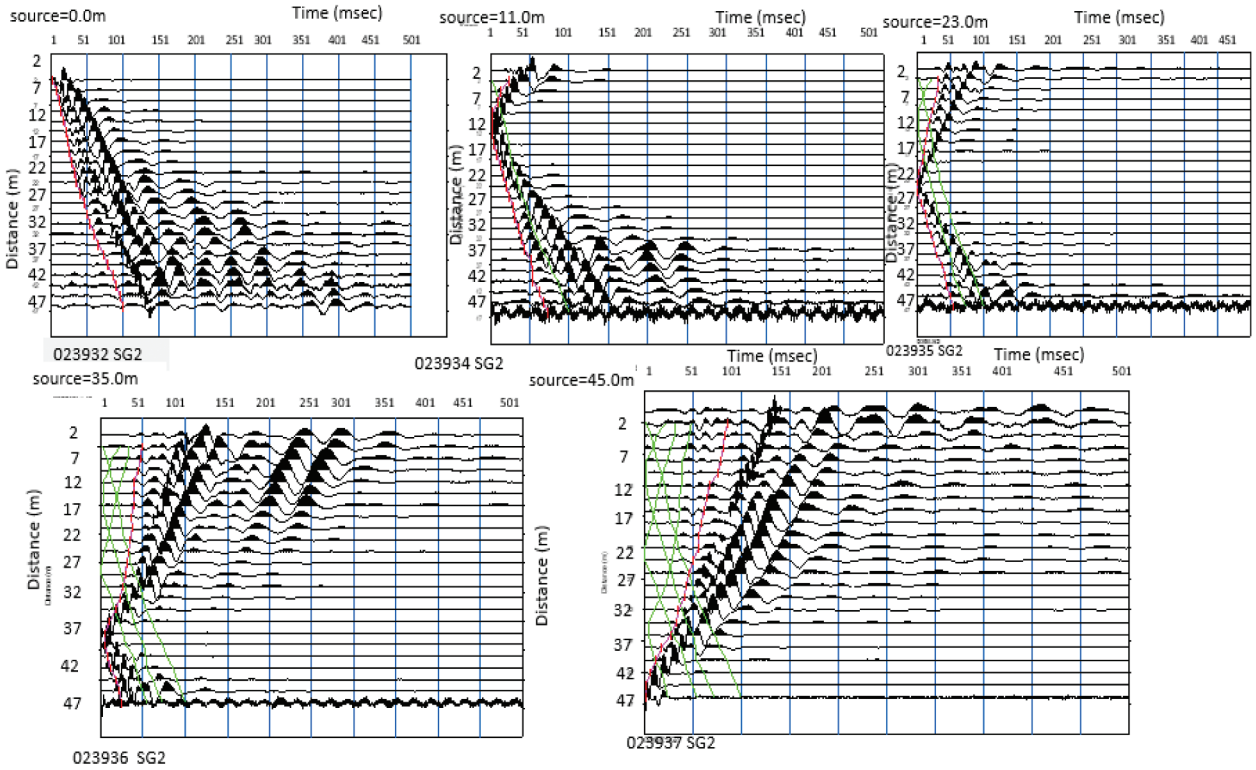

Figure 3. First breaks picking of five-shot points on Line 1 using SeisImager/2D (Pickwin module).

In recent times, highway pavement failure has been a very serious problem that causes unnecessary delays in traffic flow, distorts pavement aesthetics, breakdown of vehicles, and most significantly, causes road traffic accidents that have resulted in the loss of lives and properties amounting to millions of dollars (Jegede 2004; Ogundipe 2008). For the first time, a seismic refraction survey was deployed to elucidate the geological cause of highway failure in North-Central Nigeria. Although several of Nigeria's highways are presently experiencing varying degrees of failure, the bulk of research on the causes of the instability has been in the southwestern part of Nigeria (e.g. Adiat et al., 2017; Ganiyu et al., 2021). There is therefore a need to extend this research to other parts of the country experiencing highway failure. This will not only help to compare factors affecting highway instability in different parts of Nigeria, but it will also help to propose a regional or nationwide management strategy.

The Ajaokuta-Anyigba highway is currently undergoing a large extent of cracking, patching, potholes, and complete rippling of the asphalt layer but has not

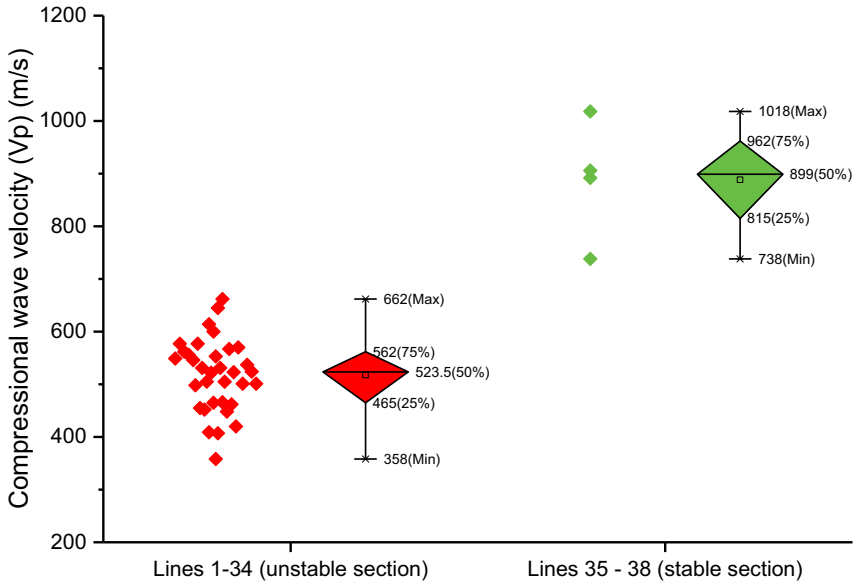

Figure 4. Box and Whisker Plots of Average P wave velocity of subgrade soils within 0–2 m depth.

Table 1. P wave velocity classification (based on geology and lithologies in trial pits).

P wave velocity (m/s)	Velocity description	Layer Assignment		Lithology	Colour code
		Lines 1–34	Lines 35–38		
300–700	low velocity	Layer 1	-	clay	yellow
700–1500	moderate velocity	Layer 2	Layer 1	weathered layer (silt/clayey sand)	green
>1500	high velocity	-	Layer 2	fresh basement	red

received any studies geared towards unravelling the causes of the highway failure. As stated earlier, the majority of studies on highway pavement failure are concentrated in the southwestern parts of Nigeria. Minimal studies on highway failure studies have been conducted in north-central Nigeria. Most of these studies involve the use of electrical geophysical methods, such as resistivity studies. Although this can provide information about the subsurface profile, the obtained resistivity values are influenced by other factors of the earth's material not related to its mechanical or elastic engineering properties. Seismic refraction has been proven to be a geophysical method that gives information that can be used to decipher the engineering properties of the subsoil. These include the stiffness, Young's modulus, shear modulus, and Poisson ratio. According to Palmtrom (1996), the closest geophysical method to rock mass engineering is the seismic refraction method.

Furthermore, important properties of foundation soils, which include water saturation, density, and Poisson ratio, can be obtained by integration of the seismic refraction method with data from well logs (Sayed et al. 2012). The competency of rock for engineering purposes has also been well determined with the combination of well log and seismic refraction (Kilner et al. 2005; Varughese and Kumar 2011). The cause of the failure of the Ajaokuta-Anyigba highway is yet to be determined and reported. The present study is therefore aimed at first imaging the soil profiles of the failed and stable sections. Second, determining the competence of subgrade soils underlying failed and stable sections of the highway based on the P wave velocity values and their geotechnical properties. Finally, establish relationships between P wave velocity values and geotechnical properties through correlation analysis.

1.1. Study area

The study area is a portion of the Ajaokuta-Anyigba Federal Highway (N7°22′30″-7°30′0″ and E06°40′30″ – 06°48′0″), Northcentral Nigeria (Figure 1). The highway is connected to two major ceramic industries and the largest cement factory in Africa (known as the Dangote Cement Industry) situated in Kogi State, North-Central Nigeria. This makes the highway congested with several hundreds of heavy-duty trucks around the ceramic companies for commercial purposes. The highway also plays a very important role in the Nigerian road network, linking the southwest geo-political zone to the Federal Capital Territory, the northern and eastern parts of the country. Geologically, the highway is underlain by Precambrian rocks of the Southwestern Basement Complex. The present study is focused on the portion of the highway that traverses through the mica-schist and granite-gneiss, thus offering the opportunity to study the role/influence of the different geology.

Table 2. P wave velocity and geotechnical properties of subgrade soils.

Subgrade Sample no	Depth (m)	Line	[a]AverageVp (m/s)	Fines (%)	Sand (%)	LL	PI	CBR unsoaked (%)	Soaked CBR (%)	% Strength loss
A1 (Pit 1)	0.5	1	553	62	36	33.8	12.7	5	3	40
A2 (Pit 1)	1.0	1	553	61	38	28.2	15.1	6	2	67
B1 (Pit 2)	0.3	12	523	61	39	24.0	24.0	9	3	67
B2 (Pit 2)	0.4	12	523	57	43	38.8	38.8	4	3	25
C1 (Pit 3)	0.6	16	546	55	45	32.9	19.5	6	2	67
C2 (Pit 3)	0.8	16	546	62	38	34.3	25.2	6	2	67
D1 (Pit 4)	0.3	20	448	55	45	29.4	23.5	8	3	63
D2 (Pit 4)	0.6	20	448	55	45	31.2	22.4	8	4	50
E1 (Pit 5)	0.2	24	452	52	48	21.3	14.3	4	3	25
E2 (Pit 5)	0.6	24	452	53	47	27.5	18.2	5	3	40
F1 (Pit 6)	0.4	28	462	55	45	31.0	20.5	9	2	78
F2 (Pit 6)	0.8	28	462	56	44	24.0	16.0	8	3	63
G1 (Pit 7)	0.5	30	549	64	36	26.3	21.2	6	4	33
G2 (Pit 7)	0.6	30	549	60	40	23.8	23.8	5	4	20
H1 (Pit 8)	0.3	31	455	64	36	38.5	18.6	6	4	33
H2 (pit 8)	0.4	31	455	64	36	46.0	17.4	8	4	50
I1 (Pit 9)	0.6	32	501	55	45	40.0	17.5	6	3	50
I2 (Pit 9)	0.8	32	501	58	42	30.0	18.4	7	4	43
J1(Pit 10)	0.1	37	738	29	71	23.2	8.1	15	7	43
J2(Pit 10)	0.5	37	738	20	80	25.5	7.3	17	8	53
K1(Pit 11)	0.5	38	892	21	77	25.0	0.4	16	10	38

[a]N.B. LL is Liquid limit; PI is Plasticity index; CBR is California Bearing Ratio. Only points where the P wave velocities values and geotechnical results of the subgrade soils co-exist are presented in this table. Others are shown in Table 1

a

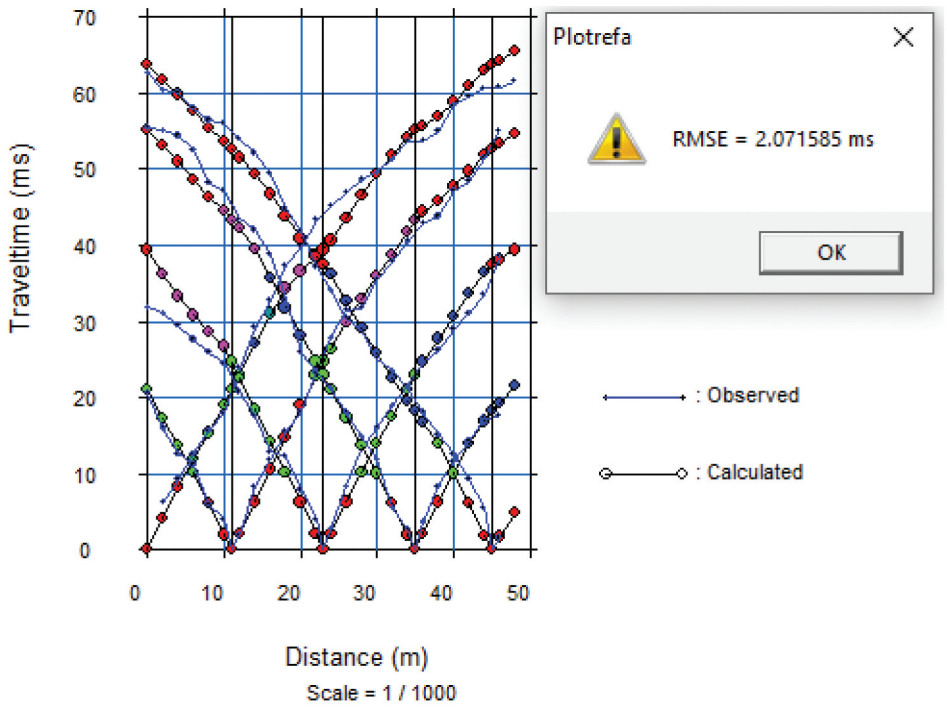

b

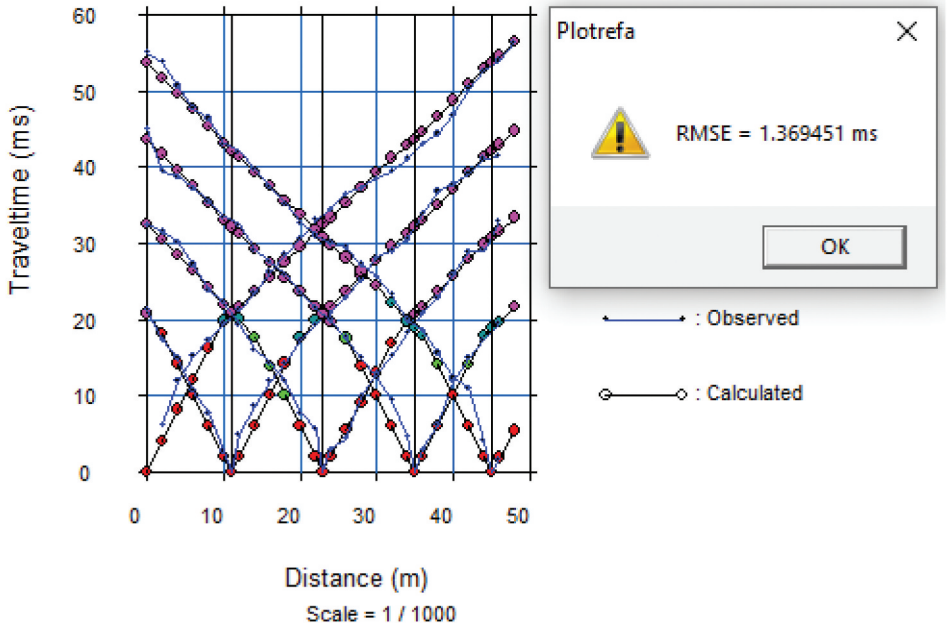

Figure 5. (a) Travel time-distance curve for line 31 (b). Travel time-distance curve for line 32 (c) Vp distribution for line 31 (d) Vp distribution for line 31 (e) Vp distribution for composite lines 31 and 32.

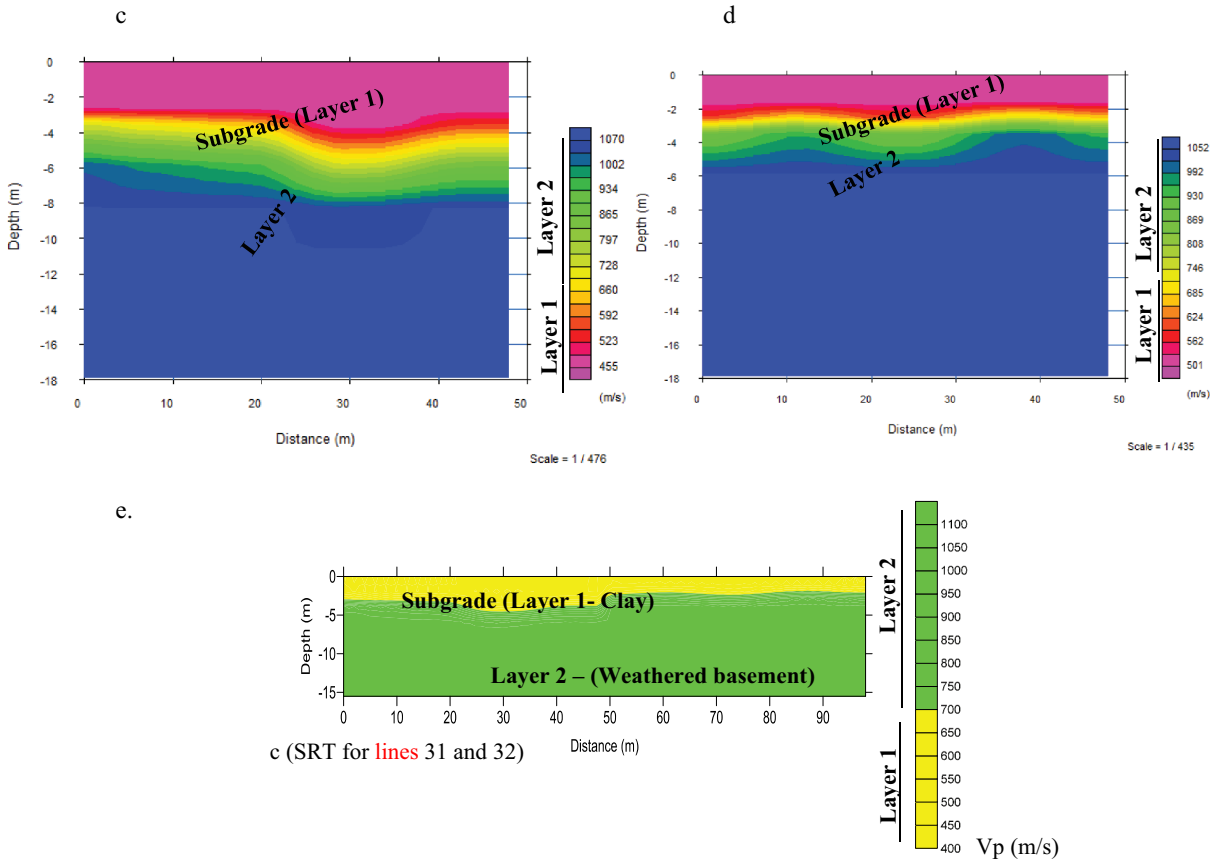

Figure 5. (Continued).

2. Methodology

Seismic refraction tomography has been adopted in this study as it can overcome the limitations of the conventional seismic refraction method in areas characterised by velocity structures with lateral and vertical velocity gradients. A total of 38 seismic refraction lines were occupied about 0.5–1 m away from the flanks of the highway. The highway was divided into two sections based on the geology, lines 1–36 are underlain by mica-schist (the unstable part of the highway), while lines 36–38 are underlain by granite-gneiss on the stable part of the highway (Figure 1). A twenty-four-channel seismograph of 10 Hz vertical geophones with 2 m spacing was adopted. Five shot points at 0 m, 11 m, 23 m, 35 m, and 45 m were used for each line as shown in Figure 2. The length of each line was 48 m. The source of the seismic wave was generated by the use of an approximately 10 kg-sledge hammer that was impacted on a thick/heavy metal plate.

Seismic Refraction Tomography (SRT) Data processing

Twenty-one bulk samples of subgrade soils were taken from eleven trial pits along the 2D seismic refraction lines. The depth of sampling ranged from 0.1–1 m. Eighteen of the subgrade samples were obtained from the failed section, while the remaining three were from the stable section. The subgrade soils were subjected to the following laboratory tests at the Department of Civil Engineering Laboratory, Federal University of Abeokuta, Nigeria:

(a) Index tests (Grain size distribution and Atterberg's limits – liquid limit and plastic limit)
(b) Strength tests (Compaction, unsoaked and soaked California Bearing Ratio)

For the grain size distribution, to disaggregate the clays that were tightly bound to the sand fractions, 2% Sodium Hexametaphosphate (Calgon) was added to the soil solution. This effectively removed the clay and silt from the sand. This procedure has also been adopted by Adeyemi and Oyeyemi (2000). Sieve analysis was then performed on the air-dried samples following the standard code by the American Society for Testing and Materials (ASTM D6913). The portion of soil that passed through the 75 microns was subjected to Atterberg's limit tests, namely, liquid limit (LL) and plastic limit (PL) according to ASTM D4318. The plasticity index (PI) was obtained by subtracting the plastic limit from the liquid limit.

A compaction test was performed on the soils using the energy of the standard proctor following ASTM D1557 to obtain the Optimum Moisture Content as well as the Maximum Dry Density. The unsoaked CBR

Table 3. P wave velocity values for Lines 1–38.

Highway condition	Rock Type	Line	Depth (m)	Range of Vp (m/s)	Average Vp (m/s)
Unstable	Mica-Schist	1	0–2 /2-4 /4-15	530–577 /577-651 /651-734	553/612/720
Unstable	Mica Schist	2	0–2 /2-4 /4-15	500–568 /530-793 /793-934	522/691/911
Unstable	Mica Schist	3	0–2 /2-4 /4-15	528–535 /535-904 /904-917	531/696/915
Unstable	Mica Schist	4	0–2 /2-4 /4-15	500–505 /505-668 /668-966	505/578/906
Unstable	Mica Schist	5	0–2 /2-4 /4-15	467–581 /581-887 /887-908	505/578/906
Unstable	Mica Schist	6	0–2 /2-4 /4-15	526–569 /569-898 /898-1077	531/706/904
Unstable	Mica Schist	7	0–2 /2-4 /4-15	607–680 /680-765 /765-952	645/720/918
Unstable	Mica Schist	8	0–2 /2-4 /4-15	573–626 /626-685 /685-721	600/654/715
Unstable	Mica Schist	9	0–2 /2-4 /4-15	436–663 /663-815 /815-1885	662/739/1350
Unstable	Mica Schist	10	0–2 /2-4 /4-15	455–761 /761-1292 /1292-1769	567/1106/1329
Unstable	Mica Schist	11	0–2 /2-4 /4-15	453–715 /715-924 /924-932	577/821/931
Unstable	Mica Schist	12	0–2 /2-4 /4-15	485–558 /558-774 /774-802	523/664/797
Unstable	Mica Schist	13	0–2 /2-4 /4-15	400–407 /407-717 /717-925	407/510/1022
Unstable	Mica Schist	14	0–2 /2-4 /4-15	460–465 /465-860 /860-1055	465/596/1022
Unstable	Mica Schist	15	0–2 /2-4 /4-15	460–466 /466-944 /944-1198	466/626/1156
Unstable	Mica Schist	16	0–2 /2-4 /4-15	530–575 /575-759 /759-866	546/665/860
Unstable	Mica Schist	17	0–2 /2-4 /4-15	522–613 /613-764 /764-818	570/679/809
Unstable	Mica Schist	18	0–2 /2-4 /4-15	550–556 /556-735 /735-1424	556/616/1290
Unstable	Mica Schist	19	0–2 /2-4 /4-15	400–409 /409-981 /981-1487	409/599/1403
Unstable	Mica Schist	20	0–2 /2-4 /4-15	440–448 /448-465 /465-1239	448/454/1072
Unstable	Mica Schist	21	0–2 /2-4 /4-15	340–358 /358-1137 /1137-1381	358/618/1340
Unstable	Mica Schist	22	0–2 /2-4 /4-15	500–568 /530-793 /793-934	501/601/735
Unstable	Mica Schist	23	0–2 /2-4 /4-15	550–562 /562-817 /817-1388	562/647/1293
Unstable	Mica Schist	24	0–2 /2-4 /4-15	398–561 /561-1202 /1202-1486	452/833/1438
Unstable	Mica Schist	25	0–2 /2-4 /4-15	572–691 /691-1079 /1079-1187	614/891/1168
Unstable	Mica Schist	26	0–2 /2-4 /4-15	465–654 /654-842 /842-1308	537/748/1075
Unstable	Mica Schist	27	0–2 /2-4 /4-15	523–630 /630-843 /843-1476	577/736/1353
Unstable	Mica Schist	28	0–2 /2-4 /4-15	450–468 /468-752 /752-1308	462/562/986
Unstable	Mica Schist	29	0–2 /2-4 /4-15	500–524 /524-1275 /1275-1477	524/806/1443
Unstable	Mica Schist	30	0–2 /2-4 /4-15	476–647 /647-794 /794-1107	549/718/1024
Unstable	Mica Schist	31	0–2 /2-4 /4-15	430–455 /455-708 /708-1071	455/539/1008
Unstable	Mica Schist	32	0–2 /2-4 /4-15	490–501 /501-821 /821-1053	501/792/1053
Unstable	Mica Schist	33	0–2 /2-4 /4-15	337–528 /528-741 /741-1173	420/655/1066
Unstable	Mica Schist	34	0–2 /2-4 /4-15	473–523 /523-572 /572-695	498/547/633
Stable	Granite-Gneiss	35	0–2 /2-4 /4-15	806–1006 /1006-1600 /1600-2610	906/1207/2009
Stable	Granite-Gneiss	36	0–2 /2-4 /4-15	1004–1032 /1032-1820 /1820-2315	1018/1437/2041
Stable	Granite-Gneiss	37	0–2 /2-4 /4-15	734–741 /741-1282 /1282-1816	738/1027/1527
Stable	Granite-Gneiss	38	0–2 /2-4 /4-15	763–1020/ 1020–1278 /1278-3080	892/1149/2179

test involved subjecting the soils compacted at the optimum moisture content to a penetration test. The soaked CBR [ASTM D1883] test was performed on the soils soaked for 24–48 hours to simulate the worst field condition possible during the ingress of water into the subgrade or flooding. All geotechnical tests followed the American Society of Testing and Materials (ASTM) International (2006) procedure.

The first breaks of the primary waves (Figure 3) were carefully picked using the Pickwin module of the SeisImager/2D software. The picked arrivals were then saved using the save pick file, which was further opened using the Plotrefa module of the same software. The travel-time graph was displayed. Layers were assigned and time-term inversion was performed. Tomographic inversion was then performed. This involves beginning with an initial velocity model and then iterating until the misfit between the observed and calculated travel times is reduced to the minimum. Finally, the 2D depth-velocity distribution for each line was generated to show the subsurface layers. The root means square error (RMS), which is the misfit between the observed and calculated data was less than 3%. Surfer 8 (Surfer 8.01 2002) software was further used to merge a set of 2 SRT lines to show the lateral variation of the subsurface lithology for about 100 m. Additional information on the step-by-step processing and interpretation of seismic refraction are documented in Al-Saigh and Al-Heety (2014), Al-Heety and Shanshal (2016), and Anukwu et al. (2020). The P wave velocity values were correlated with subsurface geology from geotechnical and trial pit results.

3. Results and discussion

According to the American Association of State Highways and Transportation Officials (AASHTO 2006), the first top 2 m are paramount to the integrity of the highway as they constitute the subgrade soil and are closest to the pavement. Therefore, the focus of the study was the subgrade soils within 0–2 m depth. The average Vp values of the subgrade soil (within depths of 0–2 m), which is the unit of interest are summarised using the box and whisker plot as shown in Figure 4.

The results show that the Vp values of the subgrade soils of the unstable section range between 358–662 m/s, while in the stable section, Vp values range between 738–1018 m/s (Figure 4). These values fall in the range of low and moderate P wave velocity, respectively (Table 1). These results suggest that the unstable sections generally

a

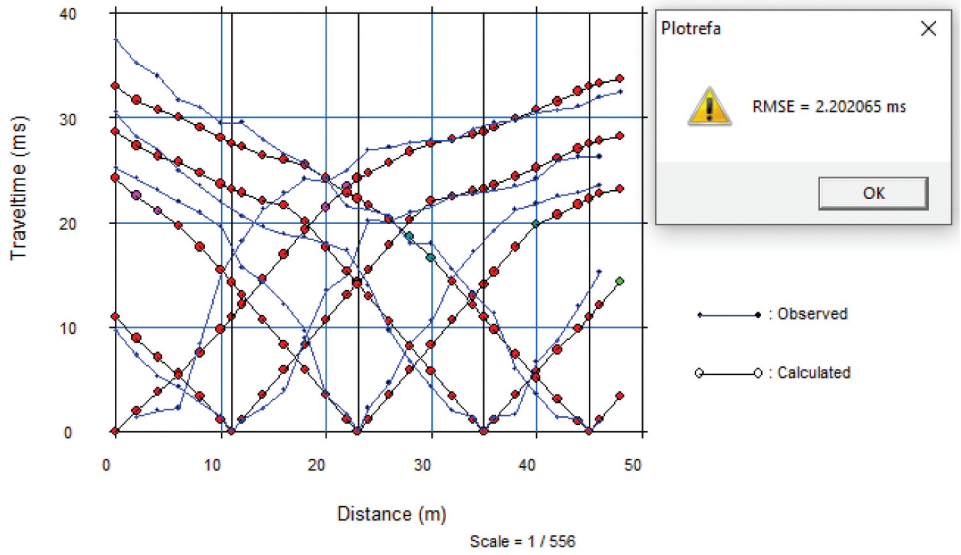

b.

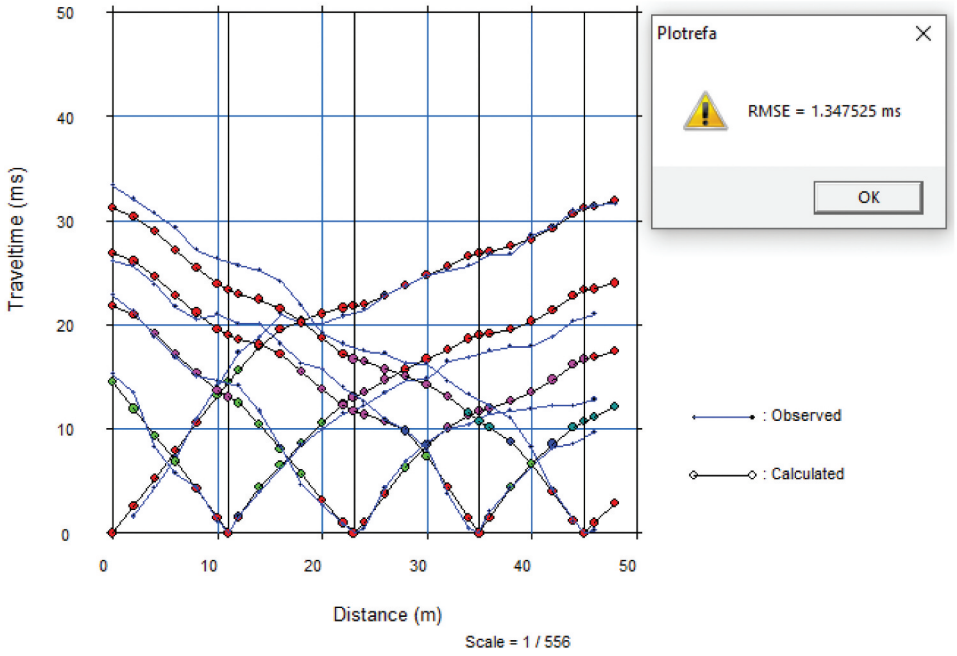

Figure 6. (a) Travel time-distance curve for line 37 (b). Travel time-distance curve for line 38 (c) Vp distribution for line 37 (d) Vp distribution for line 38 (e) Vp distribution for composite lines 37 and 38.

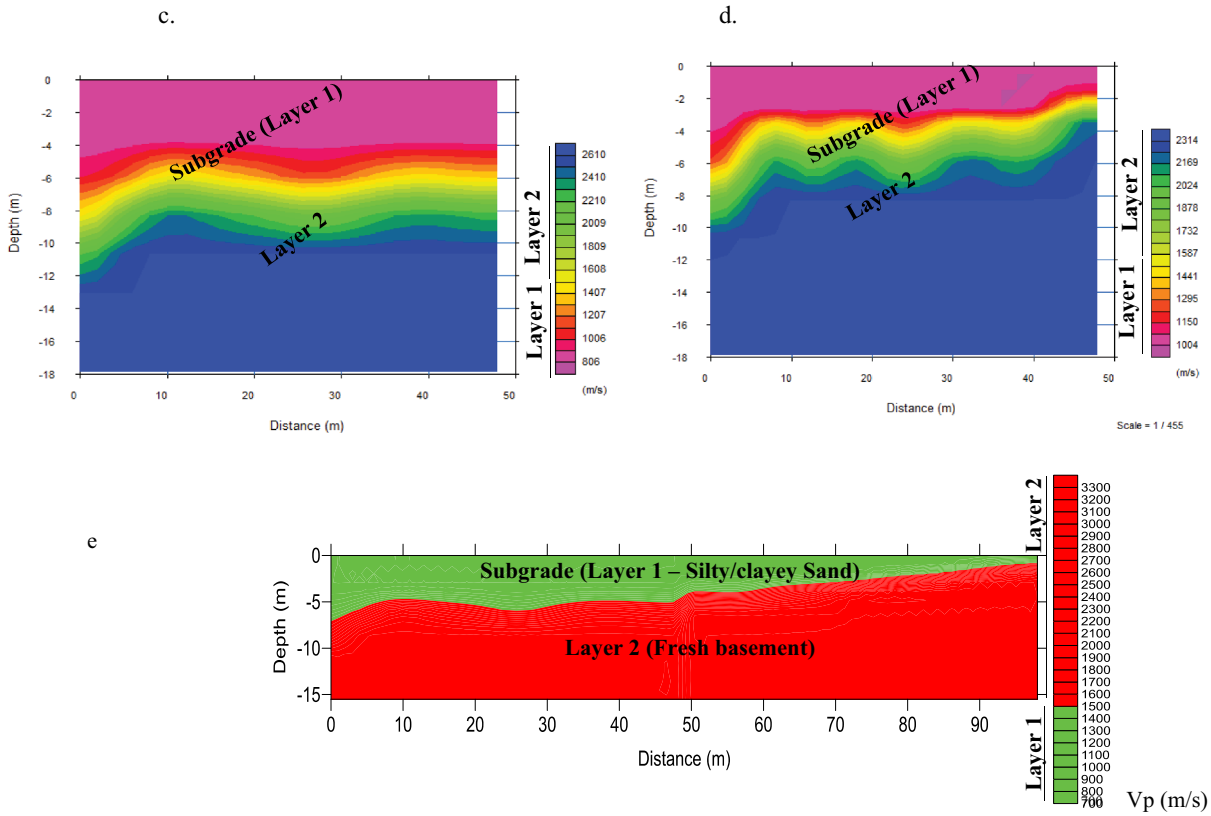

Figure 6. (Continued).

have subgrade soils that are weak and soft and thus facilitate the failure of the sections. By contrast, the subgrades of the stable section are of a moderate competency, as evidenced by their higher P wave velocity.

The geotechnical properties (grain size distribution, Atterberg limit, and CBR) of the subgrade soils obtained along both sections (Table 2) further corroborate the P wave velocity results. The subgrade soils of the unstable section have higher fines (52–64%), a lower amount of sand (36–48 %), a higher liquid limit (21.3–46.0), a higher plasticity index (12.7–38.8), lower unsoaked CBR (4–9), lower soaked CBR (2–4) and higher percentage strength loss upon soaking (20–78%) than those of the stable sections. The subgrades of the stable section have fines, sand, liquid limit, plasticity index, unsoaked CBR, soaked CBR, and percentage strength loss due to soaking ranging from 20–29%, 71–80%, 23.2–25.5, 0.4–8.1, 15–17, 7–10 and 38–53% respectively. The subgrades of the unstable section are generally classified as A-6 and A-7-6 clayey soils, with low to high plasticity, and fair to poor subgrade ratings (AASHTO 2006), whereas the subgrades of the stable section are grouped as A-2-4 silty sands with low compressibility and good to excellent subgrade ratings.

Figure 5(a-e) show the travel time-distance curves, velocity depth models from tomography, and composite lines 31 and 32 (west of the River Niger, Figure 1). Within 0–2 m, which corresponds to the depth of subgrade soils of interest, the P wave velocity values range from 430–501 m/s (Table 3), representing low velocity, weak, loose and soft subgrade clayey materials. This layer is problematic for highway stability due to the possibility of swelling and shrinkage, usually associated with clay soils. The result reflects the weathering product of the parent rock (mica-schist), which is essentially clay. Megascopic examination shows that the mica-schist consists primarily of mica (muscovite and biotite), feldspar, and small amounts of quartz. The feldspar and mica disintegrate into clay, thus giving rise to clay. Because a very minimal amount of quartz is in the parent rock, the sand in the subgrade soils is also minimal, thus offering a very little contribution to the stability. This is also supported by the geotechnical results. The subgrades of these profiles have fines, sand, liquid limit, plasticity index, unsoaked CBR, soaked CBR, and percentage strength loss due to soaking ranging from 55–64%, 36–42%, 30–46%, 17.4–18.6, 6–8, 3–4 and 33–50% respectively (Tables 2 and 3). According to the American Association of State Highways and Transportation Officials (AASHTO 2006) and the Federal Ministry of Works and Housing (FMWH, 1997), the results reveal that the soils are A-6 clayey soils with a fair to poor subgrade rating. Furthermore, the high percentage loss in strength in the subgrade upon soaking shows that the highway will be in a messy condition during flooding or continuous rainfall as there is no drainage by the flanks of the road.

NB. The average Vp values corresponding to 0–2 m (the subgrade) have been used for the box and whisker plot in Figure 4

In general, refraction lines along the unstable segment are underlain by the same parent rock (Mica-schist) (Figure 1). This rock is subjected to similar environmental conditions of weathering, thus producing subgrade soils with similar characteristics and sequences that are weak as foundation soils for highway pavement, causing highway failure. A form of soil improvement is therefore recommended. This failure is further exacerbated by several heavy-duty trucks travelling along this section day and night due to its proximity to two major ceramic industries in the state and the non-availability of drainage systems. However, depths greater than 4 m are evaluated as suitable for foundation depths for the highway pavement in rehabilitation exercises. This is because their P-wave velocity values are at these depths (651–2610 m/s) comparable to the P-wave velocity (734–1820 m/s) at lower depths (0–4 m) of the stable section underlain by Granite Gneiss (Table 1).

Figure 6(a-e) show the travel time-distance curves, velocity depth models from tomography, and composite lines 37 and 38 (to the east of River Niger – Figure 1). Within the first 2 m, the P wave velocity of the subgrade soils (the first layer) ranges from 734–1032 m/s. This range falls within the moderate P wave velocity and corresponds to a subgrade soil with a moderate level of compaction and strength. Also, this P wave velocity range is interpreted as possibly a sandy-clay subgrade (this is confirmed by the geotechnical test). The P wave velocity result reflects the weathering product of the parent rock (granite gneiss), which is sandy-clay. Megascopic examination of the granite-gneiss shows that it consists of quartz, feldspar, and mica. The quartz within the granite-gneiss being highly resistant to weathering forms sand, while feldspar and mica disintegrate into clay, thus giving rise to a sandy-clay mixture. The stability of the highway on this section points to the competency of the layer underneath the pavement. In addition, the shallow depth to the basement < 1–5 m with high P wave velocities ranging from 1816–3080 m/s also contributes significantly to the stability of the highway. Geotechnical results of the subgrade soils along these lines have fines (weight percent), sand (weight percent), liquid limit,

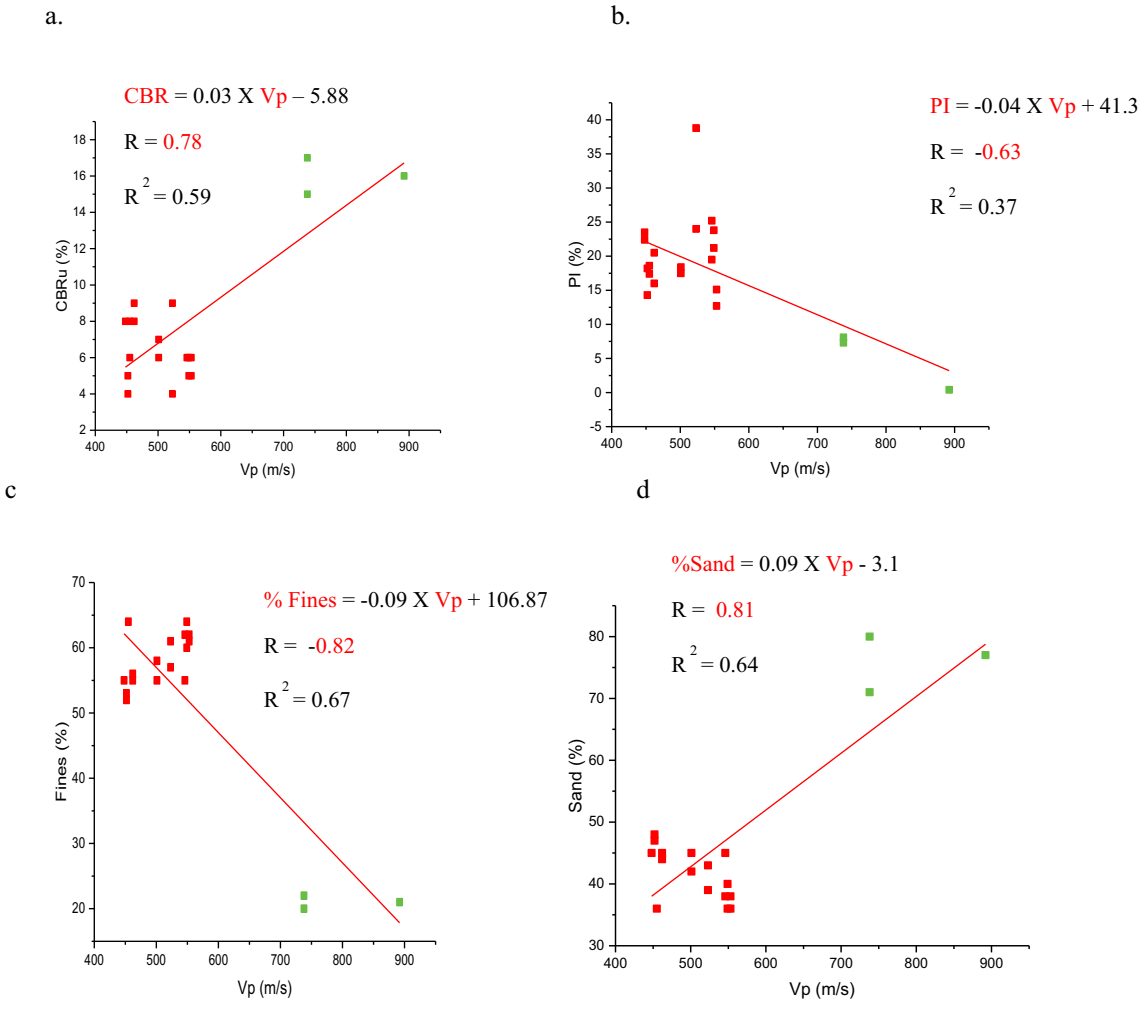

Figure 7. Regression plots of Vp with (a) CBR, (b) PI, (c) Fine (%) and (d) Sand (%).

plasticity index, unsoaked CBR, soaked CBR, and percentage strength loss due to soaking ranging from 20–29%, 71–80%, 23.2–25.5, 7.3–8.1, 15–17, 7–8 and 53%, respectively. The results reveal that the soils are A-2-4 silty/clayey sand with an excellent to good subgrade rating (AASHTO 2006; FMWH 1997). Although there would have been appreciable strength loss upon flooding, the design of the road ensured that drainage was incorporated, which took care of the anticipated negative effect.

A few studies (e.g. Umar et al. 2020 and Ige et al., 2020) conducted on sections of some failed highways in North-Central Nigeria using electrical geophysics and geotechnical studies, respectively, concluded that clayey subgrade soils are a major cause of pavement failure. This is in agreement with the present research. The current study, however, not only reveals that the clayey substratum is responsible for the failure but also provides the P wave velocity values of the subsoils. These values can in turn be integrated (in further research) with other geophysical and well log properties such as shear wave velocity and density to obtain soil dynamic parameters such as stiffness, Young's modulus, shear modulus, and Poisson's ratio, which are critical for civil engineering construction.

3.1. Correlation between P wave velocity and geotechnical parameters

Studies conducted by several authors (e.g. Adewoyin et al., 2021; Ayolabi and Adegbola 2013; Akintorinwa and Oluwole 2018; Islam et al. 2020) have shown that certain geotechnical properties may be reliably predicted from geophysical data. For instance, Ayolabi and Adegbola (2013) obtained a coefficient of correlation (R^2) of 0.97 between Share wave velocity and Standard Penetration Test N (SPT-N) value. To study the relationships between some measured geotechnical properties and P wave velocity, the results were subjected to regression analysis. The regression plots of P wave velocity against CBR, PI, fines, and sands are shown in Figure 7 (a-d). The results reveal that both CBR and sand have a fairly strong positive correlation with P wave velocity (r = 0.78 and 0.81, respectively). On the other hand, the amounts of fines and the plasticity index are negatively correlated with P wave velocity (r = – 0.82 and –0.63 respectively). This implies that P wave velocity increases with an increase in sand and CBR value while the same decreases with an increase in fines and plasticity index.

4. Conclusion

The study has shown that integrated seismic refraction tomography with geotechnical tests is suitable for evaluating subgrade soil competency in highway investigations. The P wave velocity reflected the nature of the geology underlying both sections and their degree of competence. The failed section is underlain by subgrade soils formed by the extensive weathering of mica-schist, while the stable section is underlain by weathered products of granite-gneiss. The subgrade soils of the unstable section (0–2 m depth) are characterised by clayey, weak, and soft subgrade soils with low P wave velocity, while the stable section has sandy-silt subgrade soils with moderate velocity. The subgrades of the unstable section are generally classified as A-6 and A-7-6 clayey soils, with low to high plasticity and a fair to poor subgrade rating. On the other hand, the subgrades of the stable section are grouped as A-2-4 silty sands with low compressibility and a good to excellent subgrade rating. P wave velocity increased with an increase in the amount of sand and CBR but decreased with an increase in fines and plasticity index. Thus, high amounts of fines, low amounts of sand, high plasticity index, and low P wave velocity are major contributors to the instability of the failed highway. In rehabilitation exercise, depths greater than 4 m are evaluated as suitable for foundation depths for the highway pavement. Alternatively, soil improvement is recommended for the upper (0–2 m) layer.

Acknowledgements

The authors wish to appreciate the anonymous reviewers for their significant contributions that helped to improve the quality of this paper.

Disclosure statement

No potential conflict of interest was reported by the author(s).

ORCID

Obasaju Daniel Opemipo http://orcid.org/0000-0002-5448-1386
Oloruntola Moroof http://orcid.org/0000-0001-7760-9365
Oladele Sunday http://orcid.org/0000-0001-7168-8293
Ojekunle Victor http://orcid.org/0000-0003-1405-4037
Baiyegunhi Christopher http://orcid.org/0000-0003-2748-3332

References

AASHTO. 2006. Standard specification for transportation materials and methods of sampling and testing. American Association of State Highways and Transportation Officials. 14th ed. Washington (D.C).

Adegbola RB, Ayolabi EA, Allo W. 2012. Subsurface characterization using seismic refraction and surface wave methods: a case of Lagos State University, Ojo, Lagos State. Arab J Geosci. doi:10.1007/s12517-012-0784-2

Adewoyin OO, Joshua EO, Akinwumi II, Omeje M, Joel ES. 2017. Evaluation of geotechnical parameters using geophysical data. J Eng Technol Sci. 49(1):95–113. doi:10.5614/j.eng.technol.sci.2017.49.1.6.

Adewoyin OO, Joshua EO, Akinyemi ML, Omeje M, Adagunodo TA, Joel ES. 2021. Engineering site investigations using surface seismic refraction technique. IOP Conf Series Earth Environ Sci. doi:10.1088/1755-1315/655/1/012098

Adeyemi GO, Oyeyemi F. 2000. The geotechnical basis for failure of sections of the Lagos-Ibadan expressway, southwestern Nigeria. Bull Eng Geol Environ. 59(1):39–45. doi:10.1007/s100649900016.

Adeyemi GO, Oloruntola MO, Adeleye AO. 2014. Geotechnical properties of subgrade soils along sections of the Ibadan–Ife Expressway, South-Western Nigeria. J Nat Sci Res. 4(23):67–75.

Adiat KAN, Akinlatu AA, Adegoroye AA. 2017. Evaluation of road failure vulnerability section through integrated geophysical and geotechnical studies. NRIAG J Astron Geophys. 6:245–255. doi:10.1016/j.nrjag.2017.04.006.

Aka MU, Okeke FN, Ibout JC, and Obiora DN. 2018. Geotechnical investigation of near-surface structures using seismic refraction techniques in parts of Akwa Ibom State, Southern Nigeria. Model Earth Syst Environ. 4:451–459. doi:10.1007/s40808-018-0440-2.

Akintorinwa OJ, Oluwole ST. 2018. Empirical relationship between electrical resistivity and geotechnical parameters. NRIAG J Astron Geophys. 7(1):123–133. doi:10.1016/j.nrjag.2018.02.004.

Al-Heety AJ, Shanshal ZM. 2016. Integration of seismic refraction tomography and electrical resistivity tomography in engineering geophysics for soil characterization. Arab J Geosci. 9(1):1–11. doi:10.1007/s12517-015-2116-9.

Al-Saigh NH, Al-Heety AJ. 2014. Seismic refraction tomography and MASW survey for geotechnical evaluation of soil for the teaching hospital project at Mosul University. J Zankoy Sulaimani- Part A (JZS-A). 16(1):1–14.

Allo OJ, Ayolabi EA, Oladele S. 2019. Investigation of near-surface structures using seismic refraction and multichannel analysis of surface waves methods—a case study of the University of Lagos main campus. Arab J Geosci. 12:257. doi:10.1007/s12517-019-4397-x

American Society of Testing and Materials (ASTM) International. 2006. Standard practice for classification of soils for engineering purposes (unified soil classification system). American Society for Testing and Materials. West Conshohocken. p. 12.

Anukwu GC, Khalil AE, Nawawi M, Younis MA. 2020. Delineation of shallow structures in the vicinity of Ulu Slim hot spring using seismic refraction and MASW techniques. NRIAG J Astron Geophys. 9(1):7–15. doi:10.1080/20909977.2019.1702803.

Ayolabi EA, Adegbola RB. 2013. Application of MASW in road failure investigation. Arab J Geosci. doi:10.1007/s12517-013-1078-z

Azwin IN, Saad R, Nordiana M. 2013. Applying the Seismic refraction tomography for site characterization. APCBEE Procedia. 5:227–231. doi:10.1016/j.apcbee.2013.05.039.

Federal Ministry of Works and Housing (FMWH). 1997. Nigerian general specification for roads and bridges. Federal Highway Department, FMWH: Abuja, Nigeria. 2: 145 - 284.

Ganiyu SA, Oladunjoye MA, Olobadola M, Arizebeokhai O, P A, Badmus BS. 2021. Investigation of incessant road failure in parts of Abeokuta, southwestern Nigeria using integrated geodetic methods and soil analysis. Environ Earth Sci. 80(4). doi:10.1007/s12665-021-09446-4.

Ige OO, Kuforiji SO, Olaleye MI 2020. Geophysical, Geotechnical and Mineralogical studies of a section along Ilorin-Lokoja Federal Highway, Southwestern Nigeria. Minna Journal of Geosciences. 4(2):230–244.

Ilori AO, Obianwu VI, Okwueze EE. 2014. Seismic investigation of highway pavement failures in parts of Southeastern Nigeria. J Environ Eng Geophys. 19:113–134. doi:10.2113/JEEG19.2.113.

Islam I, Ahmed W, Rashid UM, Orakzai AU, Ditta A. 2020. Geophysical and geotechnical characterization of shallow subsurface soil: a case study of University of Peshawar and surrounding areas. Arab J Geosci. 13:949. doi:10.1007/s12517-020-05947-x

Izumotani S, Takeuchi M, Murayama H, Okazaki K. 2020. Estimating rock properties using seismic refraction survey data: a case study in an abandoned road tunnel. Explor Geophys. doi:10.1080/08123985.2020.1828856

Jegede G. 2004. Highway pavement failure induced by poor geotechnical properties along a section of Okitipupa-Igbokoda highway, southwestern Nigeria. Ife J Sci. 6(1):41–44.

Kearey P, Brooks M, and Hill I. 2002. An introduction to geophysical exploration. 3rd. United Kingdom.: Blackwell publishing

Khalil HK, Hanafy S. 2016. Geotechnical parameters from seismic measurements: two field examples from Egypt and Saudi Arabia. J Environ Eng Geophys. 21(1):13–28. doi:10.2113/JEEG21.1.13.

Kilner M, West LJ, Murray T. 2005. Characterization of glacial sediments using geophysical methods for groundwater source protection. J Appl Geophys. 57(4):293–305. doi:10.1016/j.jappgeo.2005.02.002.

Mohammed AME, Abu El Ata ASA, Abdel Azim F, Taha MA. 2013. Site-specific shear wave velocity investigation for geotechnical engineering applications using seismic refraction and 2D multichannel analysis of surface waves. NRIAG J Astron Geophys. 2:88–101. doi:10.1016/j.nrjag.2013.06.012.

Ogundipe OM. 2008. Road pavement failure caused by poor soil properties along Aramoko-Ilesa highway, Nigeria. J Eng Appl Sci. 3(3):239–241.

Okigbo N. 2012. Causes of highway failures in Nigeria. Int J Eng Sci Technol. 4(11):4695–4703.

Okpoli CC, Bamidele AA. 2016. Geotechnical investigation and 2-D electrical resistivity survey of a pavement failure in Ogbagi Road, Southwestern Nigeria. Int J Sci Basic Appl Res. 2(7):47–58.

Oladapo MI, Olorunfemi MO, Ojo JS. 2008. Geophysical Investigation of road failures in the basement complex of Southwestern Nigeria. Res J Appl Sci. 3(2):103–112.

Onimisi M, Obaje NG, Daniel A. 2013. Geochemical and petrogenetic characteristics of the marble deposit in Itobe area, Kogi State, Central Nigeria. Adv Appl Sci Res. 4(5):44–57.

Optim. 2001. User's manual SeisOpt^{R}@2D^{TM} Version 2.8, Optim LLC, UNR-MS 174, 1664 N. Reno (Nevada): Virginia St.

Palmtrom A (1996). Application of seismic refraction survey in assessment of jointing. Paper published in conference on Recent Advances in Tunneling Technology, New Delhi. pp. 1–13

Pegah E, Mahmoodi M. 2016. Evaluation of Seismic hazard and site geodynamic properties by using geophysical methods in the North of Iran. J Eng Geol Constr. 5(2):126–142.

Reynolds JM. 2011. An introduction to applied and environmental geophysics. 2nd eds ed. Chichester: John Wiley and Sons Ltd.

Roodposhti HR, Hafizi MK, Kermani MRS, Nik MRG. 2019. Electrical resistivity method for water content and compaction evaluation, a laboratory test on construction material. J Appl Geophys. 168:49–58. doi:10.1016/j.jappgeo.2019.05.015.

Sayed SR, Moustafa EH, Ibrahim EE, Mohamed M, Naser AA. 2012. Seismic refraction and resistivity imaging for assessment of groundwater seepage under a dam site, Southwest of Saudi Arabia. Int J Phys Sci. 7(48):6230–6239.

Steeples DW, Miller RD. 1990. Seismic reflection methods applied to engineering, environmental and groundwater problems. Investigations in geophysics. Rev Tutorial Soc Exploit Geophys. 1(5):1–30.

Surfer 8.01. 2002. Surface-mapping system. Colorado U.S.A: Golden Software Incorporation.

Umar MU, Ejepu JS, Aweda AK, Ozoji TM, Adamu LM, Abdulkad SA, Umoru CI. 2020. A multi-dimensional approach to revealing causes of pavement failures: a case study of Mina Suleja highway, North-central Nigeria. Am J Water Sci Eng. 6(3):81–88. doi:10.11648/j.ajwse.20200603.11.

Varughese A, Kumar N (2011). Seismic refraction survey a reliable tool for subsurface characterization for hydropower projects. Proceedings of Indian Geotechnical Conference, Kochi, India, pp137–139